

# Characteristics of Nitrogen and Sulfur Double Doping in Mahogany Wood-Based Porous Carbon for Potential Carbon Capture Application

Annisa Aprilia<sup>1,\*</sup>, Shofwah Rihadatul Aisy<sup>2</sup>, Noto Susanto Gultom<sup>1</sup>, Ayi Bahtiar<sup>1</sup>

<sup>1</sup>Physics Department, Faculty of Mathematics and Natural Sciences, Universitas Padjadjaran, Jl. Ir. Soekarno KM 21, Jatinangor, Kabupaten Sumedang, 45363, West Java, Indonesia.

<sup>2</sup>Physics Study Program, Faculty of Mathematics and Natural Sciences, Universitas Padjadjaran, Jl. Ir. Soekarno KM 21, Jatinangor, Kabupaten Sumedang, 45363, West Java, Indonesia.

\*Author to whom correspondence should be addressed:

E-mail: a.aprilia@phys.unpad.ac.id

(Received October 23, 2024; Revised April 24, 2025; Accepted May 14, 2025)

**Abstract:** Mahogany (*Swietenia macrophylla king*) wood residue has the potential to serve as a raw material for the synthesis of porous carbon due to its relatively high biomass content. This study examines the effects of N-S doubly dopant agents on the physicochemical properties of porous carbon that is derived from mahogany wood debris. The doping operations utilizing thiourea and the activation using KOH are conducted simultaneously. We found that dual doping with N and S influences the porosity of the resultant porous carbon. Our sample with a 1:2 ratio of raw material to thiourea (PC-2) has the highest specific surface area of 870.78 m<sup>2</sup>/g and pore volume of 0.552 cm<sup>3</sup>/g among all as-prepared samples. The activation process results in the formation of carbon porosity. The number and size of pores are both increased by N-S heteroatom co-doping, which leads to an increase in surface area. During the carbonization process, unreacted N-S heteroatoms are eliminated. This results in the formation of a carbon matrix with a distinctive structure that contains two N and S dopants.

**Keywords:** mahogany wood waste; N-S doped; one-step carbonization; porous carbon

## 1. Introduction

Global warming issues occur continuously, and their impacts escalate yearly, causing increasing temperatures over time that can alter the climate and natural balance<sup>1,2</sup>. Industrial activities are primarily responsible for the rising atmospheric carbon dioxide (CO<sub>2</sub>) levels, contributing to most global warming<sup>3</sup>. Since industrial activities cannot be halted for production purposes, implementing carbon capture technology can be an alternative to reducing CO<sub>2</sub> concentrations in the atmosphere. Researchers have reported several chemical processes for carbon capture and storage (CCS), which use adsorbents to selectively bind CO<sub>2</sub> molecules<sup>4,5</sup>. CCS is an important technology that directly captures CO<sub>2</sub> from source points and atmospheric air. Sustainable chemical processes, such as thermal conversion and photo/electrochemical reduction of CO<sub>2</sub>, can utilize the captured CO<sub>2</sub> to produce materials and chemicals<sup>5,6</sup>. The famous CO<sub>2</sub> capture methodology is by adsorption process due to high efficiency, selectivity to

certain substances, lower energy consumption, and the high opportunity for industry utilization<sup>7,8</sup>. Since carbon dioxide (CO<sub>2</sub>) gas is acidic, the adsorbent must have a porous surface and possess chemical properties suitable for enhancing selectivity towards this substance. The capacity for adsorption and its chemical structure significantly influence how materials interact with polar and nonpolar adsorbates. Activated carbon derived from biomass exhibits promising properties as a carbon capture and storage (CCS) active material. Its porous morphology provides numerous active sites, such as edges, dislocations, and discontinuities, which are crucial in facilitating chemical reactions with other atoms<sup>9,10</sup>.

The molecule of CO<sub>2</sub> has an activation energy to dissociate the double bond between carbon and oxygen (O=C=O), which is relatively high (532 kJ mol<sup>-1</sup>); thus, particular research is essential to develop effective material as a capture agent<sup>4</sup>. The chemical structure of activated carbon is an essential characteristic of the CO<sub>2</sub> adsorption mechanism. The insertion of nitrogen (N) and sulfur (S) into the carbon framework has been reported to enhance

CO<sub>2</sub> adsorption behavior through acid-base interactions, electrostatic interactions, and hydrogen bonding<sup>11</sup>). Nitrogen has a comparable atomic size to carbon, allowing it to substitute carbon atoms in the carbon skeleton easily<sup>12</sup>). The electronegativity of nitrogen (3.04) is higher than carbon (2.55), which provides more active sites such as pyridinic-N, pyrrolic-N, graphitic-N, and oxidized-N, thereby substantially improving the adsorption capabilities of carbon materials. Doping with nitrogen will inject numerous electrons into the carbon matrix, resulting in increased conductivity. It has been reported by other researchers that nitrogen doping of the carbon matrix induces structural changes and alters surface chemistry, thereby enhancing the number of adsorptive sites<sup>13</sup>). Sulfur functional groups in the carbon matrix enhance the electron density of the carbon grid surface, which can improve both wettability and surface reactivity<sup>14</sup>). Thiourea (CH<sub>4</sub>N<sub>2</sub>S) can be used as a dopant to obtain simultaneous N and S doping<sup>15</sup>). N and S dopants derived from thiourea on activated carbon have been shown to improve electrochemical properties, which are also associated with an increase in specific surface area<sup>14</sup>).

Plantation waste has the potential to become activated carbon because this biomaterial has a relatively high biomass content. *Swietenia macrophylla* King (Mahogany wood) has a biomass content of around 54.07%. The trunk of the mahogany tree is composed of cellulose, hemicellulose, lignin, and extractive substances, with a majority consisting of carbon. In Indonesia, mahogany wood is abundantly available and widely used in the furniture and construction industries due to its low cost<sup>16</sup>). The biopolymer structure of wood inherently includes cellulose, hemicellulose, and lignin, with mahogany wood specifically comprising 25.82% lignin, 47.26% cellulose, and 47.21% hemicellulose<sup>17</sup>). Due to its high lignin content, mahogany wood is considered a promising precursor for producing porous carbon. The research on CO<sub>2</sub> capture material-based porous carbon with nitrogen and sulfur double doping has been actively pursued in recent years and still needs further investigation<sup>18</sup>). The same doping elements in the carbon source can produce different characteristics that relate to the synthesis parameters and the natural ingredients of the raw carbon source<sup>19,20</sup>). Therefore, this study aims to explore the influence of co-doping nitrogen and sulfur introduced by thiourea on the physical characteristics of porous carbon derived from mahogany wood waste. Specifically, this research aims to determine how variations in the mass ratio between thiourea and biomass affect key properties such as surface area, pore volume, and pore diameter. The ultimate goal is to optimize the synthesis conditions to produce porous carbon materials with excellent physicochemical properties for potential CO<sub>2</sub> adsorption applications.

## 2. Materials and Methods

The raw material used in this study was leftover mahogany wood from sawmills with an average diameter of 1 mm. The mahogany sawdust (MS) was obtained from a production site that manufactures household furniture in the local area. First, the raw material was washed using deionized water. After soaking in ethanol, the MS was completely dried in an electric oven. KOH was used as activator agent in this study with a KOH: MS ratio of 1:1, while thiourea as the source of N and S dual doping. KOH activator and thiourea as a dopant were dissolved simultaneously in deionized water. The variations of the ratio between MS and thiourea are (1:0), (1:0.5), and (1:1). The mixture was then sonicated for 30 minutes and stirred for 2 hours. Subsequently, the mixture was filtered using filter paper and dried on a hot plate for 36 hours at 85°C. The identification (providing sample code) for each mass ratio variation is shown in Table 1. The carbonization was conducted using a one-step pyrolysis method at 700°C under N<sub>2</sub> gas flow<sup>21</sup>). The dry powder was placed in an alumina boat and inserted into a tube furnace, then heated gradually until 700°C with a heating rate of 5°C per minute for 2 hours under a nitrogen atmosphere. After pyrolysis, the furnace was allowed to cool naturally to room temperature under continuous N<sub>2</sub> flow. The resulting carbon was washed several times with deionized water until neutral pH was achieved. To remove residual potassium and enhance porosity, samples were rinsed with 0.1–0.5 M HCl<sup>22,23</sup>). The purified carbon was then dried, crushed, and sieved to obtain a fine carbon powder suitable for characterization.

## 3. Results and Discussion

Table 1 shows the variation of the ratio between mahogany sawdust (MS), activator (KOH), thiourea, and yield of carbon mass that resulted, calculated from the percentage ratio of carbon and raw material mass. The type of activator influences the degradation of glucose and fructose. Since KOH is a base, fragmentation reactions occur, forming glyceraldehyde, glycolaldehyde, erythrose, dihydroxyacetone, and pyruvaldehyde, reducing charcoal formation and decreasing yield. Lignin, cellulose, and hemicellulose decomposition decrease the carbon mass produced. Additionally, increasing thiourea concentration decreases the yield of porous carbon. According to Luo et al., this may be due to the reduced use of carbon sources in the mahogany sawdust as raw material and the collapse of pore structures during activation<sup>24</sup>). Figure 1 shows the picture of all samples. The PC-1 samples have almost the same volume as the others, but the yielding of carbon mass is lower than the others.

We observed the morphology and microstructural analysis of all samples using a scanning electron microscope (SEM), as shown in Figure 2. The carbon that has not yet

been activated and carbonated commonly has smooth surfaces without pores<sup>21,25</sup>. Figure 2(a) shows the sample morphology after activation and carbonation without thiourea doping (PC-0). The reaction caused by KOH as an activator generates pore development, producing a sponge-like structure. KOH is mainly used as an activator to produce carbon pores and has already been reported<sup>21</sup>. After adding thiourea doping (Figure 2b-d), the porous carbon surface exhibits more dense pore structures with reduced size. These results indicate that adding nitrogen and sulfur sources can significantly enhance the formation of porous carbon structures. The use of nitrogen (N) as a dopant in carbon structures has been reported to disrupt carbon bonds, as shown by C. Kim et al. Their study demonstrated that nitrogen doping promotes the formation of micropores, likely due to defect sites generated by structural distortions within the carbon framework<sup>26</sup>. Similarly, research by N. Abeladi et al. found that nitrogen-containing additives in biocarbon not only act as structure-directing agents (porogens) but also contribute to the expansion of pore size into the mesoporous range<sup>27</sup>. Research by J. Bai et al. indicates that sulfur (S) helps suppress the structural rearrangement of carbon during pyrolysis, thereby leading to a more amorphous and porous carbon material<sup>28</sup>. This results in a high specific surface area, which is essential for effective gas adsorption. These findings suggest that nitrogen and sulfur functions not only as a dopant but also plays a critical role in the development of porosity in carbon materials.

**Table 1:** The variation of the ratio between mahogany sawdust (MS), activator (KOH), thiourea, and yield of carbon mass

Sample code	Ratio of MS:KOH:Thiourea	Carbon mass (g)	Yield (%)
PC-0	(1:1:0)	3.8	47.55
PC-0.5	(1:1:0.5)	2.56	36.61
PC-1	(1:1:1)	0.73	9.09
PC-2	(1:1:2)	3.16	31.59

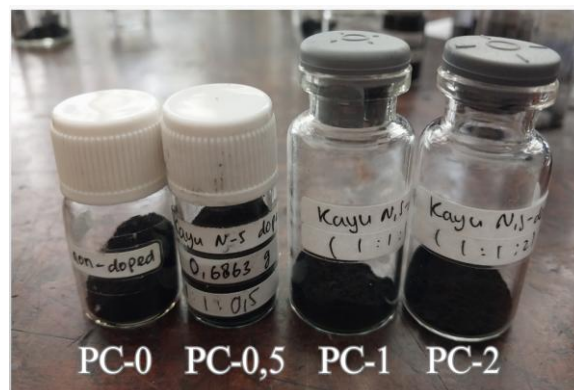
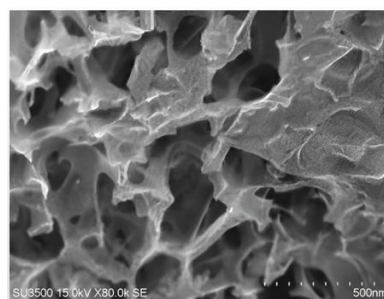
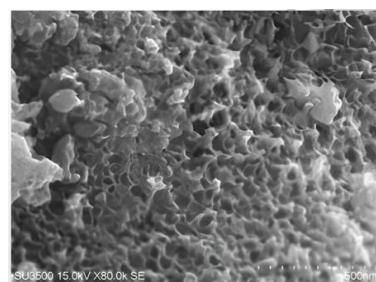


**Fig. 1:** Photographs of porous carbon resulted from this research. The MS mass is different for each one: 8g, 7g, 8g, and 10g for PC-0, PC-0.5, PC-1, and PC-2, respectively

The sample elemental composition was given in Table 2 and compared to the raw material. The activated process increased carbon's weight percentage (wt%) and reduced other elements, such as oxygen and nitrogen. The nitrogen in the raw material originates naturally from organic complex compounds such as protein and amino acids. Nitrogen is typically contained in the side chains of these molecules<sup>29</sup>. The activation process involves heating carbon in an activating gas at high temperatures, which can result in eliminating non-carbon components such as hydrogen, oxygen, and nitrogen from the carbon raw material. Heating at high temperatures causes the loss of many volatile substances in the material and the occurrence of oxidation compounds<sup>26</sup>. This can also be influenced by the pH of the activator used, as the resulting reactions release water in the porous carbon.



(a)



(b)

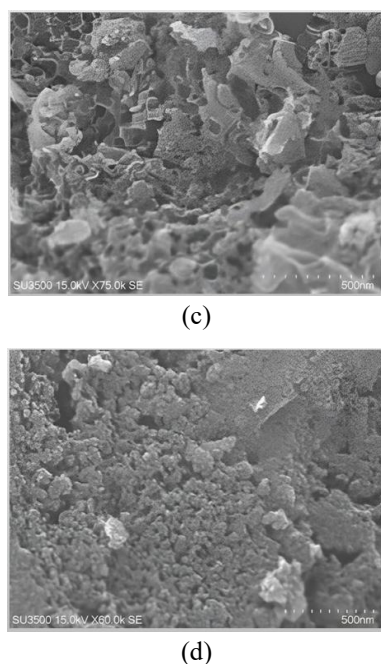


**Fig. 2:** Porous carbon morphology with and without N-S doping (a) PC-0, (b) PC-0.5, (c) PC-1, (d) PC-2

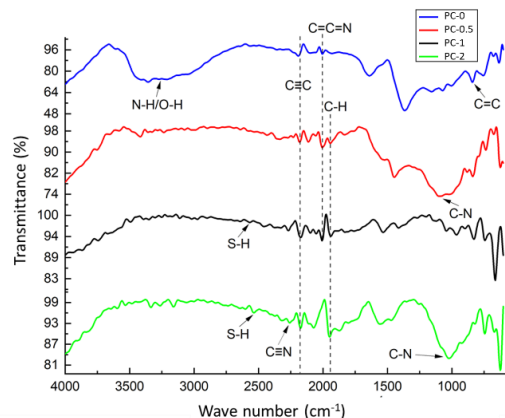
An excessive dose of thiourea makes the pores on the carbon surface smaller and tends to be invisible (Figure 2d). According to Table 2, the PC-2 sample has the highest sulfur content. The presence of sulfur can affect the pore formation process in activated carbon during activation<sup>21,30</sup>. Sulfur can alter the carbon structure through substitution of carbon atoms. Excessive sulfur incorporation may lead to significant changes in the pore structure, as sulfur atoms replace carbon atoms. This substitution reduces the available pore volume and specific surface area due to the larger atomic radius of sulfur compared to carbon. The adsorption properties of activated carbon are influenced by pore size distribution and pore volume<sup>31,32</sup>. Nitrogen doping can modify its surface characteristics—particularly by increasing surface acidity—which in turn affects the pore structure and adsorption behavior. This enhanced surface acidity is strongly correlated with the graphitization of carbon resulting from nitrogen doping<sup>33</sup>.

Figure 3 shows the FTIR spectra for the samples. All porous carbons exhibit the same  $\text{C}\equiv\text{C}$  peak (2190-2260  $\text{cm}^{-1}$ ). The PC-0, PC-0.5, and PC-1 samples have the same peak at  $\text{C}=\text{C}=\text{N}$  (2000  $\text{cm}^{-1}$ ). The PC-0 sample contains  $\text{C}=\text{C}$  (790-840  $\text{cm}^{-1}$ ) and  $\text{N}-\text{H}/\text{O}-\text{H}$ . After thiourea doping, the PC-0.5 sample contains  $\text{C}-\text{N}$  (1020-1250  $\text{cm}^{-1}$ ) and  $\text{C}-\text{H}$  (1650-2000  $\text{cm}^{-1}$ ). The PC-1 sample contains  $\text{C}-\text{H}$  (1650-2000  $\text{cm}^{-1}$ ) and  $\text{S}-\text{H}$  (2550-2600  $\text{cm}^{-1}$ ). The PC-2 sample contains  $\text{C}-\text{N}$  (1020-1250  $\text{cm}^{-1}$ ),  $\text{C}-\text{H}$  (1650-2000  $\text{cm}^{-1}$ ),  $\text{C}\equiv\text{N}$  (2222-2260  $\text{cm}^{-1}$ ), and  $\text{S}-\text{H}$  (2550-2600  $\text{cm}^{-1}$ ). The PC-0.5 sample has the highest N content compared to the PC-0, PC-1, and PC-2 samples. The PC-0.5 sample

did not detect any bonds between sulfur due to its low concentration. The formation of bonds between N and S with other elements proves that the porous carbon was effectively doped with the heteroatoms N and S.

**Table 2:** Elemental compositions of all samples

Sample	Elements			
	C (wt%)	O (wt%)	N (wt%)	S (wt%)
MS	36.87	46.91	16.23	0
PC-0	54.32	45.36	0.32	0
PC-0.5	63.08	26.84	6.93	3.15
PC-1	65.80	23.42	1.94	8.84
PC-2	69.62	3.62	6.28	20.48



**Fig. 3:** Fourier Transform Infrared spectra of all samples

XPS analysis was conducted further to investigate the samples' surface chemical properties and to demonstrate thiourea's role in the surface chemical composition. The XPS spectra for the PC-0 sample and its analysis are shown in Figure 4. The spectrum consists of two peaks; the first is the main peak at 284.6 eV, which belongs to the  $\text{sp}^2$  graphite lattice. The second, at 286.4 eV, originates from the  $\text{C}-\text{O}$  bond. The nitrogen spectrum is not identified due to the low nitrogen content and the sample not being doped. The oxygen spectrum consists of three peaks. The two main peaks at 531.8 and 533.4 eV originate from the  $\text{O}-\text{C}=\text{O}$  and  $\text{C}=\text{O}$  bonds, respectively. The peak at 535.4 eV arises from the  $\text{C}-\text{O}$  bond. The XPS spectra for the PC-0.5 sample are shown in Figure 5. The survey spectrum shows the presence of peaks from  $\text{OC}1\text{s}$ ,  $\text{O}1\text{s}$ , and  $\text{N}1\text{s}$ . In the carbon  $\text{C}1\text{s}$  spectrum, the main peak at 284.6 eV belongs to the  $\text{sp}^2$  graphite lattice, and the peak at 285.4 eV is due to the  $\text{C}-\text{O}$  bond. The oxygen spectrum consists of three peaks<sup>34</sup>. The two main peaks at 531 and 532.2 eV originate from the  $\text{O}-\text{C}=\text{O}$  and  $\text{C}=\text{O}$  bonds, respectively, while the peak at 535.3 eV originates from the  $\text{C}-\text{O}$  bond

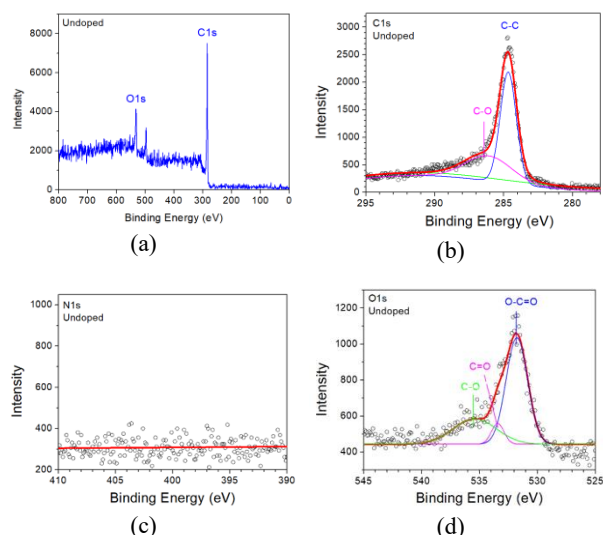


**Fig. 4:** (a) XPS spectrum of PC-0 (undoped), (b) C1s spectrum, (c) N1s spectrum, (d) O1s spectrum

The nitrogen spectrum of PC-0.5 is divided into two peaks at 398.3 and 400 eV, classified as pyridinic-N and pyrrolic-N functional groups, respectively. This indicates that nitrogen element was detected in the porous carbon sample. N doping will introduce more electrons into the carbon matrix, thereby increasing conductivity<sup>35,36</sup>. Additionally, N doping will generate more active sites. Pyridinic-N can act as a catalyst in redox reactions and influence the electronic properties of activated carbon material. At the same time, pyrrolic-N can enhance the adsorption capacity of activated carbon for gases such as CO<sub>2</sub>. Pyrrolic-N possesses a lone pair of electrons on nitrogen that can engage with CO<sub>2</sub> molecules via van der Waals forces and electrostatic interactions<sup>37</sup>. This interaction can increase the adsorption capacity of activated carbon for CO<sub>2</sub>.

The sulfur spectrum also contains two peaks at 163.4 and 168.4 eV, which can be classified as S-C and oxidized-S functional groups<sup>37</sup>. This indicates that S doping can be detected in the double-doped N, S porous carbon sample. The functional group of sulfur in the carbon matrix increases the electron density on the carbon grid surface, enhancing wettability and surface activity. Oxidized-S functional groups have a high affinity for CO<sub>2</sub> because they can interact with the charge of CO<sub>2</sub>. Additionally, oxidized-S groups can form hydrogen bonds with CO<sub>2</sub>, enhancing their interaction. This interaction enables strong CO<sub>2</sub> adsorption on the surface of the porous carbon material, thereby enhancing the material's ability to capture CO<sub>2</sub>. The added nitrogen and sulfur functions alter the electronic structure and density of the carbon, contributing not only to inducing CO<sub>2</sub> interaction but also to providing pseudocapacitance activity<sup>25</sup>. Oxygen is associated with residual structural oxygen from starch, atmospheric moisture, and CO<sub>2</sub>. According to Nazir et al., the increased binding energy of oxidized-S and pyrrolic-N with CO<sub>2</sub>

molecules contributes to the strong affinity of N and S-doped adsorbents for CO<sub>2</sub>, ultimately leading to greater CO<sub>2</sub> adsorption<sup>30</sup>. The observed peaks from bonds between C, N, and S indicate that N, S-doped carbon has been successfully synthesized.

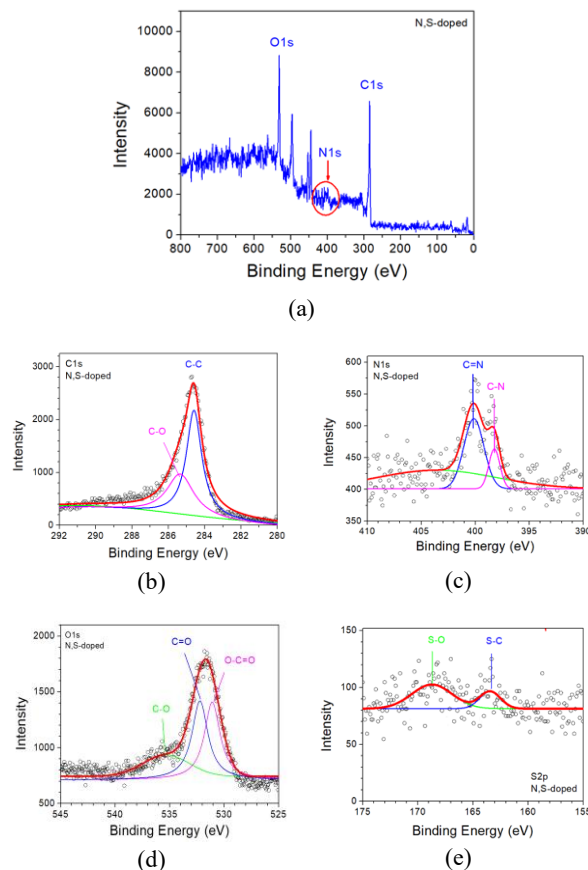


**Fig. 5:** (a) XPS Spectrum of N, S doped (PC-0.5), (b) C1s spectrum single bond, (c) N1s spectrum, (d) O1s spectrum, (e) S2p spectrum

Porous size distribution was determined using a DFT method from BET measurement at P/P<sub>0</sub> = 0.0-1.0, as shown in Figure 6. Table 3 lists the surface area, pore volume, and the average pore size of our modified carbon. The surface area incrementally increases as porosity develops. The highest surface area of 870 m<sup>2</sup>/g is achieved with the PC-2 sample. Based on Figure 6, the decrease in N<sub>2</sub> adsorption in PC-0.5 suggests that this sample has a limited surface area. The PC-0.5 sample contains a high nitrogen content but low sulfur content. While nitrogen increases the number of pores, sulfur penetrates the carbon matrix effectively, as noted by L. Zhao et al.<sup>38</sup>. This may lead to the formation of numerous pores with larger diameters, ultimately reducing the total pore volume. The relatively large average pore diameter in PC-0.5 results in greater void space within the porous carbon structure. Luo et al.<sup>24</sup> reported that porous carbon derived from distillation waste with dual N and S doping exhibited a decrease in specific surface area as the thiourea dose



increased. The reduction in total pore volume may also be attributed to material redistribution within the pore structure, which can limit the available space<sup>39</sup>). Additionally, changes in pore size distribution and modifications in pore structure may occur due to interactions between thiourea and carbon. Although the specific surface area initially decreases in PC-0.5, it later increases in the PC-1 and PC-2 samples. The increase in N<sub>2</sub> adsorption of porous carbon doped with N and S is due to the enhancement of the pore structure environment resulting from the addition of N and S dopants into the carbon<sup>40</sup>). This situation can improve the porosity by gradually removing heteroatoms to achieve greater porosity and specific surface area. Enhanced thiourea doping can optimize surface porosity by altering the amount of thiourea in the polymer solution, producing a unique structure consisting of carbon matrix containing dual elements N and S.

**Table 3:** Porous textural of all samples

Sample	Porous textural		
	S <sub>A</sub> BET (m <sup>2</sup> /g)	V <sub>ave</sub> (cm <sup>3</sup> /g)	d <sub>ave</sub> (nm)
PC-0	159.38	0.133	3.34
PC-0.5	83.62	0.129	6.15
PC-1	425.93	0.283	2.66
PC-2	870.78	0.552	2.54

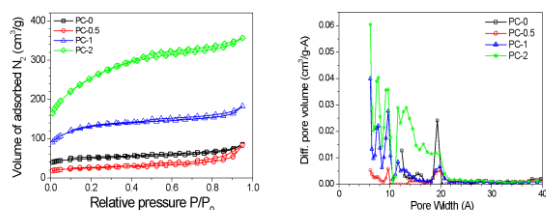


**Fig. 6:** (a) N<sub>2</sub>-adsorption-desorption isotherms and (b). Pore size distribution of the samples PC-0, PC-0.5, PC-1 and PC-2

#### 4. Conclusions

We have successfully prepared N, S-doped carbon utilizing Mahogany wood waste as through a one-step carbonization method. KOH was employed as the chemical activating agent, while thiourea served as the nitrogen and sulfur source. SEM/EDS analysis revealed the formation of pores with varying sizes across all samples, confirming the successful synthesis of porous carbon. Functional groups related to nitrogen and sulfur doping were identified as C–N (1020–1250 cm<sup>-1</sup>) and S–H (2550–2600 cm<sup>-1</sup>) through FTIR analysis. Further confirmation by XPS indicated the presence of C=N, C–N, S–C, and S–O bonds, with binding energies of 398.3, 400, 163.4, and 168.4 eV, respectively. The incorporation of

nitrogen and sulfur dopants significantly enhanced the textural properties of the carbon material. An increase in doping levels led to a noticeable rise in both surface area and pore volume. Among all samples, PC-2 exhibited the highest performance, with a surface area of 870.78 m<sup>2</sup>/g and a pore volume of 0.552 cm<sup>3</sup>/g, indicating its strong potential for CO<sub>2</sub> capture applications.

#### Acknowledgments

This work was financially supported by an Internal Research Grant from Universitas Padjadjaran through the Academic Research Grant (ALG) Scheme, under contract No. 1549/UN6.3.1/PT.00/2023, dated March 27, 2023.

#### Nomenclature

CO <sub>2</sub>	Carbon dioxide
wt%	Weight percent
KOH	Kalium hidroksida
eV	Electronvolt (1eV = 1.60218 10 <sup>19</sup> Joule)
N	Nitrogen
S	Sulfur
C	Carbon
O	Oxygen
MS	Mahogany sawdust
S <sub>A</sub> BET	Surface area from BET (m <sup>2</sup> /g)
V <sub>ave</sub>	Volume average (cm <sup>3</sup> /g)
d <sub>ave</sub>	Diameter pore average (nm)

#### Subscripts

BET	Brunauer-Emmett-Teller
ave	Average

#### References

- 1) T.M. Letcher, "Climate Change", 3rd Edition, Elsevier, 2021. doi:10.1016/B978-0-12-821575-3.00001-3
- 2) L. E. Kristie, J. Vanos, J. W. Baldwin, J. E. Bell, D. M. Hondula, N. A. Errett, K. Hayes, C. E. Reid, S. Saha, J. Spector, and P. Berry, "Extreme Weather and Climate Change: Population Health and Health System Implications", *Annu. Rev. Public Health*, 42 293-315 (2021). doi:10.1146/annurev-publhealth-012420-105026
- 3) L.J. R. Nunes, "The Rising Threat of Atmospheric CO<sub>2</sub>: A Review on the Causes, Impacts, and Mitigation Strategies", *Environments*, 10 (66) (2023). doi:10.3390/environments10040066
- 4) C. Kim, N. T. Siddulu, and L. Dai, "Electrochemical conversion porous carbon materials for CO<sub>2</sub> capture. storage and electrochemical conversion", *Materials Report: Energy*, 3(2) 100199 (2023). doi:10.1016/j.matre.2023.100199.
- 5) O.A. Olusola, U. M. Helen, R. O. Oluwatayo, R. O. Chinemerem, A. A. Christianah, and A. O. Peter, "Adsorbent technologies and applications for carbon

- capture, and direct air capture in environmental perspective and sustainable climate action”, Sustainable Chemistry for Climate Action, 3 100029 (2023). doi:10.1016/j.scca.2023.100029
- 6) I.Sullivan, A. Goryachev, I. A. Digdaya, X. Li , H. A. Atwater , D. A. Vermaas, and C. Xiang, “Coupling electrochemical CO<sub>2</sub> conversion with CO<sub>2</sub> capture”, Nature Catalysis, 4 952-958 (2021). doi:10.1038/s41929-021-00699-7
- 7) S.Acevedo., L. Giraldo., and J. C. Moreno-Piraján, “Adsorption of CO<sub>2</sub> on Activated Carbons Prepared by Chemical Activation with Cupric Nitrate”. ACS Omega, 5 (18) 10423–10432 (2020). doi:10.1021/acsomega.0c00342
- 8) X.Y. Debbie Soo, J. J. Cheng Lee, Wen-Ya Wu , L. Tao , C. Wang , Q. Zhu, and Jie Bu, “Advancements in CO<sub>2</sub> capture by absorption and adsorption: A comprehensive review”, Journal of CO<sub>2</sub> Utilization, 81 102727 (2024). doi:10.1016/j.jcou.2024.102727
- 9) R.C. Bansal and M. Goyal, “Activated Carbon Adsorption”, Taylor & Francis, 1st Edition (2005). doi:10.1201/9781420028812
- 10) H. Jedli, M. Almonnef, R. Rabhi, M. Mbarek, J. Abdessalem, and K. Slimi, “Activated Carbon as an Adsorbent for CO<sub>2</sub> Capture: Adsorption, Kinetics, and RSM Modeling”, ACS Omega, 9 2080-2087 (2024). doi:10.1021/acsomega.3c02476.
- 11) W.Shi, J. Yu, H. Liu, D. Gao, A. Yuan, and Chang B., “Hierarchically Nanoporous Carbon for CO<sub>2</sub> Capture and Separation: Roles of Morphology. Porosity. and Surface Chemistry”, ACS Applied Nano Materials, 6(9) 7887–7900 (2023). doi:10.1021/acsanm.3c01040
- 12) F.Liu, J. Niu, X. Chuan, and Y. Zhao, “Nitrogen and phosphorus Co-doped porous carbon: Dopant, synthesis, performance enhancement mechanism and versatile applications”, Journal of Power Sources, Vol. 601 234308 (2024). doi:10.1016/j.jpowsour.2024.234308
- 13) A.Grimm, G. Simoes dos Reis, S. G. Khokarale, S. Ekman, E. C. Lima, S. Xiong, and M. Hultberg, “Shiitake spent mushroom substrate as a sustainable feedstock for developing highly efficient nitrogen-doped biochars for treatment of dye-contaminated water”, Journal of Water Process Engineering, 56 (2023). doi:10.1016/j.jwpe.2023.104435
- 14) Y.Chen,dR. Hui, J. Qi, Y. Sui, Y. He, Q. Meng, F. Wei, and Y. Ren, “Sustainable synthesis of N/S-doped porous carbon sheets derived from waste newspaper for high-performance asymmetric supercapacitor”, Material Research Express, 6 (9) 095605 (2019). doi:10.1088/2053-1591/ab2d97
- 15) S. Wahyudi, J. A. Azis, F. Faizal, and A. Bahtiar, “Improved mercury ions (Hg<sup>2+</sup>) detection by composite silver nanoparticles (AgNPs) and nitrogen - Sulfur co-doped carbon dots (N, S-CDs)”, Results in Materials, 21 100551 (2024). doi:10.1016/j.rinma.2024.100551.
- 16) L.K. Hendinata, N A Siddiq A. I., R. Fikri, M. A Suprpto, and R. Prilia, “Wood-Based Energy-Saving Windows: Utilization of Transparent Wood From Mahogany Timber for Structural Applications” The proceeding of the 6th International Conference on Management of Technology, Innovation, and Project, (2023), ISSN: 1961-984X
- 17) S.Kadarwati, T Qurrochman, C Kurniawan, Jumaeri and Kasmui, “Feasibility study on the utilization of mahogany (*Swietenia macrophylla* king) wood as a raw material in the bio-oil production”, J. Phys.: Conf. Ser. 1567 022029 (2020). doi:10.1088/1742-6596/1567/2/022029
- 18) H.Cui, J. Xu, J. Shi, N. Yan, C. Zhang, S., You N., “S co-doped carbon spheres synthesized from glucose and thiourea as efficient CO<sub>2</sub> adsorbents”, Journal of the Taiwan Institute of Chemical Engineers 138 104441 (2022). doi:10.1016/j.jtice.2022.104441
- 19) K.Malini, D. Selvakumar, and N.S Kumar, “Activated carbon from biomass: Preparation, factors improving basicity and surface properties for enhanced CO<sub>2</sub> capture capacity – A review”, Journal of CO<sub>2</sub> Utilization, 67 102318 (2023), doi:10.1016/j.jcou.2022.102318
- 20) G.Singh, K. S. Lakhi, S. Sil, Sheshanath V. Bhosale, InYoung Kim, K. Albahily, and A. Vinu, “Biomass derived porous carbon for CO<sub>2</sub> capture”, Carbon, 148 164-186 (2019). doi:10.1016/j.carbon.2019.03.050
- 21) Y.Sun,K.Li, J. Zhao, J. Wang, N. Tang, D. Zhang, T. Guan, and Z. Jin, “Nitrogen and Sulfur Co-Doped Microporous Activated Carbon Macro-Spheres for CO<sub>2</sub> Capture”, Journal of Colloid and Interface Science 526 174–183 (2018). doi:10.1016/j.jcis.2018.04.101
- 22) V.Benedetti, E. Cordioli, F. Patuzzi, and M. Baratieri, “CO<sub>2</sub> Adsorption Study on Pure and Chemically Activated Chars Derived From Commercial Biomass Gasifiers”, Journal of CO<sub>2</sub> Utilization, 33 46–54 (2019). doi:10.1016/j.jcou.2019.05.008
- 23) J.Zhang, J. Shao, Q. Jin, X. Zhang, H. Yang, Y. Chen, S. Zhang, and H. Chen, “Effect of deashing on activation process and lead adsorption capacities of sludge-based biochar”, Science of the Total Environment, 716 137016 (2020). doi:10.1016/j.scitotenv.2020.137016
- 24) L. Luo, C. Yang, F. Liu, and T. Zhao, “Heteroatom-N, S Co-Doped Porous Carbons Derived From Waste Biomass as Bifunctional Materials for Enhanced CO<sub>2</sub> Adsorption and Conversion”, Separation and Purification Technology, 320 124090 (2023).

- doi:10.1016/J.SEPPUR.2023.124090
- 25) C. Ma, J. Bai, M. Demir, X. Hu, S. Liu, and L. Wang, "Water Chestnut Shell-Derived N/S-Doped Porous Carbons and Their Applications in CO<sub>2</sub> Adsorption and Supercapacitor", *Fuel*, 326 125119 (2022). doi:10.1016/j.fuel.2022.125119
  - 26) C. Kim, K. Kim, and J. H. Moon, "Highly N-doped microporous carbon nanospheres with high energy storage and conversion efficiency", *Scientific Reports*, 7 14400 (2017). doi: 10.1038/s41598-017-14686-1
  - 27) N. Abeladi, and R. Mokaya, "Modulating the porosity of N-doped carbon materials for enhanced CO<sub>2</sub> capture and methane uptake", *Journal of Material Chemistry A*, 12 21025 (2024). doi: 10.1039/d4ta03273j
  - 28) J. Bai, J. Shao, Q. Yu., M. Demir, B. Nazli Altay, T. M. Ali, Y. Jiang, L. Wang, and X. Hu, "Sulfur-Doped porous carbon Adsorbent: A promising solution for effective and selective CO<sub>2</sub> capture", *Chemical Engineering Journal*, 479 147667 (2024). doi:10.1016/j.cej.2023.147667
  - 29) N. Li, Lv Jie, and N. Deng-Ke, "Low Contents of Carbon and Nitrogen in Highly Abundant Proteins: Evidence of Selection for the Economy of Atomic Composition", *J. Mol. Evol*, Springer, 68 248-255 (2009). doi:10.1007/s00239-009-9199-4
  - 30) G. Nazir, A. Rehman, and S-J. Park, "Role of heteroatoms (nitrogen and sulfur)-dual doped corn-starch based porous carbons for selective CO<sub>2</sub> adsorption and separation", *Journal of CO<sub>2</sub> Utilization*, 51 101641, (2021). doi:10.1016/j.jcou.2021.101641
  - 31) K. Gergova, N. Petrov, and S. Eser, "Adsorption properties and microstructure of activated carbons produced from agricultural by-products by steam pyrolysis", *Carbon*, 32(4) 696-702 (1994). doi:10.1016/0008-6223(94)90091-4
  - 32) J. Dı 'az-Tera'n, D. M. Nevskaia, A. J. Lo'pez-Peinado, and A. Jerez, "Porosity and adsorption properties of an activated charcoal", *Colloids and Surfaces A: Physicochemical and Engineering Aspects*, 187-188 167-175 (2001). doi:10.1016/S0927-7757(01)00622-7
  - 33) M. Gonzales-Hourcade, G. Simoes dos reis, A. Grimm, V. M. Dinh, E. C. Lima, S. H. Larsson, and F. C. Gentili, "Microalgae biomass as a sustainable precursor to produce nitrogen-doped biochar for efficient removal of emerging pollutants from aqueous media", *Journal of Cleaner Production*, 348 131280 (2022). doi:10.1016/j.jclepro.2022.131280
  - 34) D. J. Morgan, "Comments on the XPS Analysis of Carbon Materials", *C Journal of Carbon Research*, 7 51 (2021). doi:10.3390/c7030051
  - 35) Z. Zhong, S. Mahmoodi, D. Li, and S. Zhong, "Electrochemical Performance and Conductivity of N-Doped Carbon Nanotubes Annealed under Various Temperatures as Cathode for Lithium-Ion Batteries", *Metals*, 12(12) 2166 (2022). doi:10.3390/met1212166
  - 36) X. Ren, H. Li, J. Chen, L. Wei, A. Modak, H. Yang, and Q. Yang, "N-doped porous carbons with exceptionally high CO<sub>2</sub> selectivity for CO<sub>2</sub> capture", *Carbon*, 114 473-481, (2017). doi:10.1016/j.carbon.2016.12.056
  - 37) C. H. Chang, "Preparation and Characterization of Carbon-Sulfur Surface Compounds", *Carbon*, 19 175-186 (1981). doi:0008-6223/81/030175-12S02.00/0
  - 38) L. Zhao, L. Zhao, Y. Zhao, B. Zhang, G. Liu, P. Zhang, "Nitrogen-sulfur dual-doped citric-acid porous carbon as host for Li-S batteries", *Alexandria Engineering Journal*, 31 5343-5350 (2022). doi:10.1016/j.aej.2021.10.053
  - 39) S. Li, X. Tan, H. Li, Y. Gao, Q. Wang, G. Li, and M. Guo, "Investigation on pore structure regulation of activated carbon derived from sargassum and its application in supercapacitor", *Scientific Report*, 12 10105 (2022). doi:10.1038/s41598-022-14214-w
  - 40) T. J. Badosz, M. Seredych, E. Rodríguez-Castellon, Y. Cheng, L. L. Daemen, and A. J. Ramírez-Cuesta, "Evidence for CO<sub>2</sub> reactive adsorption on nanoporous S- and N-doped carbon at ambient conditions", *Carbon*, 96 856-863 (2016). doi:10.1016/j.carbon.2015.10.007